# Energy transfer in solid solutions ZnxMg1−xWO4

**ARTICLE** *in* OPTICAL MATERIALS · AUGUST 2014

Impact Factor: 1.98 · DOI: 10.1016/j.optmat.2013.12.039

Optical Materials xxx (2014) xxx–xxx

Contents lists available at ScienceDirect

Optical Materials

journal homepage: www.elsevier.com/locate/optmat

# Energy transfer in solid solutions $Zn_xMg_{1-x}WO_4$

D. Spassky [a,b,*], S. Omelkov [a], H. Mägi [a], V. Mikhailin [b,c], A. Vasil'ev [b], N. Krutyak [c], I. Tupitsyna [d], A. Dubovik [d], A. Yakubovskaya [d], A. Belsky [e]

[a] Institute of Physics, University of Tartu, Riia 142, Tartu 51014, Estonia
[b] Skobeltsyn Institute of Nuclear Physics, M.V. Lomonosov Moscow State University, Moscow 119991, Russia Federation
[c] Physics Department, Moscow State University, Leninskie Gory 119991, Russia Federation
[d] Institute for Scintillation Materials, NAS of Ukraine, Kharkiv 61001, Ukraine
[e] Institute of Light and Matter, CNRS, University Lyon1, Villeurbanne 69622, France

ARTICLE INFO

*Article history:*
Available online xxxx

*Keywords:*
Zinc tungstate
Magnesium tungstate
Solid solutions
Luminescence
Energy transfer
Scintillating bolometers

ABSTRACT

It is shown that the light output of $Zn_xMg_{1-x}WO_4$ solid solutions has a maximum at $x = 0.5$ under X-ray excitation. Excitation spectra of exciton emission under vacuum ultraviolet excitation also show the increase of the probability of exciton creation by the geminate e–h pairs for the intermediate values of $x$. Numerical simulation of the relaxation of hot electrons and holes demonstrates that the observed effects are due to the decrease of the mean distance between thermalized charge carriers.



## 1. Introduction

An enhancement of scintillation light yield can be achieved by the transition from pure compounds to solid solutions of inorganic insulators. This effect has been shown recently for several compounds, e.g. $(Lu_xY_{1-x})AlO_3$:Ce [1], $Y_3(Al_xGa_{1-x})_5O_{12}$:Ce [2], $(Lu_xGd_{1-x})_2SiO_5$:Ce [3], $(Lu_xSc_{1-x})BO_3$:Ce [4], $(Lu_xGd_{1-x})_3(Al_yGa_{1-y})_5O_{12}$:Ce [5], $BaBr_{2-x}I_x$:Eu [6], $(Lu_xY_{1-x})BO_3$:Eu [7], CsBrI [8], $Lu_3Al_{5-x}Sc_xO_{12}$ [9]. One of the possible explanations of the observed enhancement is the decrease of the thermalization length of hot charge carriers at the stage of energy relaxation after the absorption of excitation quanta [1]. The decrease of thermalization length is supposed to be due to non-uniform distribution of substituted ions with the formation of clusters constructed from one of the component or due to the modulation of the bottom of conduction band and of the top of valence band by electronic states of randomly distributed substituted ions [1]. In both cases the increase of the efficiency of recombination and energy transfer to the emission centers can be achieved. Most of the solutions mentioned above are doped with rare earth ions. Rare-earth ions were often chosen to achieve high light yield and fast response. However the solid solutions with the dopant emission are not optimal for the study of the effect of thermalization length modification. The effect may be masked by the following effects, which also influence the efficiency of dopant emission in the solid solutions: (I) Location of the dopant energy levels within the forbidden gap depends on the concentration of one component $x$. For instance in $Gd_3(Al_xGa_{1-x})_5O_{12}$:Ce the lowest 5d state of $Ce^{3+}$ moves very close to the bottom of conduction band or even into the conduction band, when $x$ value approaches 0 [10,11]. In this case the emission of $Ce^{3+}$ ion is quenched due to the thermal ionization of the emission center. (II) Dopants are sometimes incorporated inhomogeneously into solid solutions due to the mismatch in the ionic radii of dopant and substituted cations. For instance in case of $(Lu_xY_{1-x})AlO_3$:Ce cerium ions (ionic radius of $Ce^{3+}$ = 1.143 Å) occupy rather $Y^{3+}$ (ionic radius = 1.02 Å) sites rather than $Lu^{3+}$ (ionic radius = 0.98 Å) sites. (III) Phase composition might vary with the ratio of components of a solid solution. For instance the second phase is found in $(Lu_xY_{1-x})BO_3$:Eu for $x > 0.5$, and its presence substantially modifies the energy transfer processes [7].

In order to study modification of energy transfer processes in solid solutions exclusively as a function of thermalization length of charge carriers we have to avoid the influence of all mentioned effects and choose solid solutions with the following properties: (I) Emission centers should be of intrinsic origin, e.g. emission of self-trapped excitons (STE). In case of the STE emission the process of energy transfer to the emission centers implies the efficiency of exciton creation from separated electrons and holes. (II) The parentage of the states responsible for the intrinsic emission should not be affected by the changing composition of the solid solution. (III) Solid solutions with a single phase should be selected. Solid solutions of $Zn_xMg_{1-x}WO_4$ meet all of these requirements. $ZnWO_4$

* Corresponding author at: Institute of Physics, University of Tartu, Riia 142, Tartu 51014, Estonia. Tel.: +7 495 939 3169; fax: +7 495 939 2991.
*E-mail address:* deris2002@mail.ru (D. Spassky).

0925-3467/$ - see front matter © 2014 Elsevier B.V. All rights reserved.
http://dx.doi.org/10.1016/j.optmat.2013.12.039

and $MgWO_4$ crystals belong to the wolframite type of crystal structure (space group $C_{2h}$) and demonstrate intensive luminescence due to emission of excitons self-trapped on $WO_6$ complexes. Recent calculations of the band structure demonstrated only negligible contribution from ***s*** electronic states of Mg and Zn cation in the formation of the bottom of the conduction band [12–15]. The solid solutions $Zn_xMg_{1-x}WO_4$ are also interesting for potential applications, since $ZnWO_4$ and $MgWO_4$ are considered as perspective scintillators for cryogenic scintillating bolometers [16,17].

In the present paper we have studied the dependence of exciton creation efficiency in $Zn_xMg_{1-x}WO_4$ on the relative concentration of the cations, which is determined by the value of $x$. The numerical simulation of exciton production under VUV excitation has been performed in order to demonstrate that the observed dependence of luminescence excitation spectra on $x$ is determined by the modification of thermalization length. The influence of the exciton creation efficiency on the light output under X-ray excitation has been studied as well.

## 2. Experimental details

Solid-phase synthesis method was used to obtain the charge for the single crystal growth. Initial oxides for the charge were ZnO (99.995%), MgO (99.95%) and $WO_3$ (99.995%). The crystals were grown by Czochralski method from platinum crucibles using the high-frequency heating. The growth has been carried out on the seed of $ZnWO_4$ single crystal, which was oriented along the direction [0 1 0]. As a result the set of single crystals were grown with general formula $Zn_xMg_{1-x}WO_4$ where $x$ = 0.3, 0.4, 0.5, 0.6, 0.7, 0.8, 0.9, 1. Phase composition was controlled by X-ray phase analysis and single phase of wolframite was detected in all of the grown crystals. Ratio between Zn, Mg and W in the crystals has been controlled using the scanning electron microscopy. $MgWO_4$ single crystal was grown from the melted flux solution by pulling on the rotating seed from the platinum crucible [17]. $Na_2WO_4$ was used as a solvent during the growth. The concentrations of contaminating impurities were determined by atomic emission spectral analysis. The data on the impurities detected in the investigated samples are summarized in Table 1.

The relative light output was measured on the special test bench for the samples with 2 mm thickness under X-ray irradiation (anode voltage 200 kV, current 1 mA). A laboratory set-up was used for the measurements of luminescence spectra under X-ray excitation as well as of luminescence excitation spectra and decay curves under UV radiation (photon energies 3.5–5.5 eV). Measured excitation spectra have not been corrected for the instrument function of this set-up. For some of the studied samples the measurements of luminescence excitation spectra were performed using synchrotron radiation in UV and VUV energy regions at the SUPERLUMI station (energy region 3.7–20 eV) at DESY (Hamburg) [18] and at the branch-line FINEST (energy region 15–45 eV) at MAX-lab, Lund [19]. In these cases the measured spectra were corrected using sodium salicylate. All measurements have been carried out at the room temperature on the freshly cleaved plane surfaces of the samples, which correspond to the crystallographic plane {0 1 0}.

**Table 1**
The concentration of contaminating impurities in the $Zn_xMg_{1-x}WO_4$ according to the data of atomic emission spectral analysis presented in weight ppm.

| $x$ | Impurities concentration (ppm) | | | | | | | |
|---|---|---|---|---|---|---|---|---|
| | Fe | Si | Cr | Sn | Ni | Mo | Pb | Al |
| 1 | 2 | 5 | 2 | <2 | 1 | 10 | 1 | 2 |
| 0.9 | 2 | 5 | 2.5 | <2 | 1 | 5 | 10 | 2 |
| 0.8 | 2 | 5 | 2 | <2 | <1 | 10 | <1 | 4 |
| 0.7 | 1.5 | 10 | 2 | <2 | <1 | 10 | 10 | 5 |
| 0.6 | 0.8 | 5 | 2 | <2 | <1 | 5 | <1 | 2 |
| 0.5 | 1 | 5 | 2.5 | <2 | <1 | 5 | <1 | 2 |
| 0.4 | 1 | 10 | <2 | <2 | 2 | <2 | <1 | 2 |
| 0.3 | 1 | 10 | <2 | <2 | 2 | <2 | <1 | 1 |
| 0 | 10 | 10 | <2 | <2 | 2 | <2 | <1 | <1 |

## 3. Experimental results

The luminescence spectra of $Zn_xMg_{1-x}WO_4$ under X-ray excitation are presented in Fig. 1. The observed single band peaking at 495 nm is connected with the STE emission [20]. The maximum and the width of emission band are almost independent on the value of $x$. The characteristic decay times are of few tens of μs. These values slightly increase with the decrease of $x$ from 28 μs for $ZnWO_4$ ($x$ = 1) to 35 μs for $Zn_{0.5}Mg_{0.5}WO_4$ ($x$ = 0.5) and up to 39 μs for $MgWO_4$ ($x$ = 0) under excitation in the region of direct creation of STEs ($E_{ex}$ = 4.1–4.4 eV). Therefore the characteristics of STE emission are similar for all studied crystals indicating insignificant influence from electronic states of substituted cations on the STE excited and relaxed states. It also confirms the negligible contribution of cation electronic states on the formation of the energy bands in the vicinity of the bandgap, which was predicted by band structure calculations [12–15].

The data on the light output under X-ray excitation are presented in Fig. 2. For the samples with $x$ = 0.3 and 0.8 measurements were not performed because the size of grown boules did not allow to cut the samples with the dimensions required for the test bench. The gradual increase of the light output is observed for the solid solutions with the maximum at $x$ = 0.5. For the crystal with $x$ = 0.5 the light output is increased in ~1.5 times relatively to $ZnWO_4$ and in ~2.1 times relatively to $MgWO_4$. The data on the relative scintillation light output under α-particles excitation are also presented for $MgWO_4$ and $ZnWO_4$ according to [21] and they are in a good correspondence to the values of relative light output obtained by us. Taking into account that the absolute value of scintillation light yield of $ZnWO_4$ is 21,500 ph/MeV [22], the light yield up to ~32,000 ph/MeV may be expected for $Zn_{0.5}Mg_{0.5}WO_4$ at room temperature. Since the tungstates attract attention as scintillators, the opportunity of the light yield enhancement for their solid solutions is very tempting.

Obtained results demonstrate that the increase of light output in the solid solutions is a characteristic not only for RE-doped compounds (see Section 1) but also for compounds with intrinsic STE

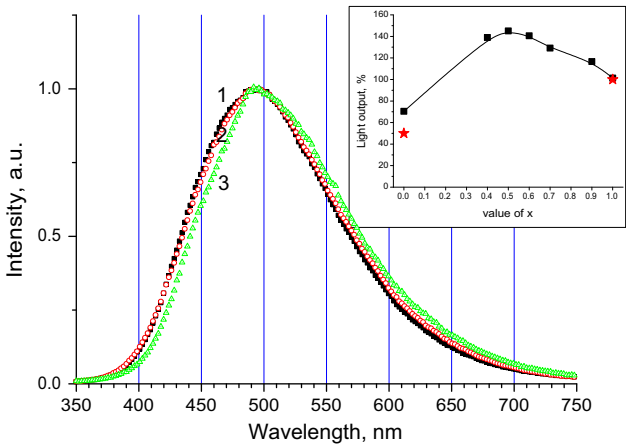


**Fig. 1.** Emission spectra of $Zn_xMg_{1-x}WO_4$ under X-ray excitation for $x$ = 1 (curve 1), 0.5 (curve 2) and 0 (curve 3). In the inset: light output of $Zn_xMg_{1-x}WO_4$ under X-ray excitation. Data on the relative scintillation light output of $MgWO_4$ and $ZnWO_4$ under excitation with α-particles are presented with circles according to [21].

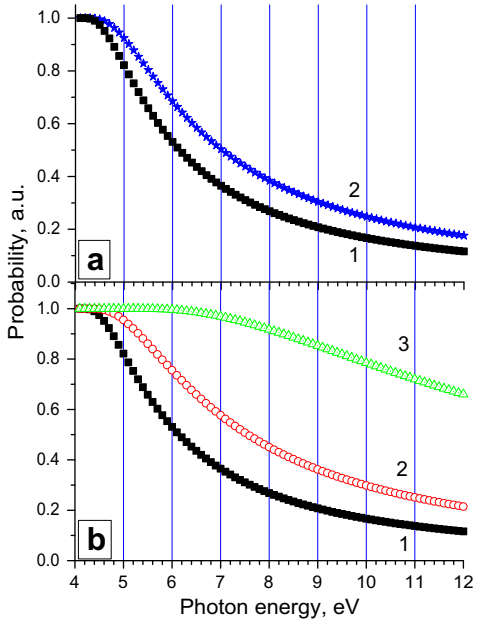


**Fig. 2.** (a) Probability of the exciton creation from geminate e–h pairs calculated for $ZnWO_4$ (curve 1) and $MgWO_4$ (curve 2). (b) Probability of the exciton creation calculated for thermalization length corresponding to the case of $ZnWO_4$ (curve 1) and for the thermalization length reduced by factor of 2 (curve 2) and 10 (curve 3).

emission. The increase, which has been detected previously for RE-doped compounds, has been attributed to the reduction of distances between thermalized electrons and holes. This hypothesis can be verified with the help of numerical simulation, which includes the thermalization length as a parameter. The probability of geminate recombination of an e–h pair $p(\hbar\omega)$ can be calculated using the Onsager model [23,24]:

$$p(\hbar\omega) = \int_0^\infty f(r, l_{eh}(\hbar\omega))(1 - e^{-R_{Ons}/r})dr$$
$$= 1 - \frac{3}{8\pi}\sqrt{\frac{3}{2}}\frac{R_{Ons}^3}{l_{eh}^3(\hbar\omega)} G_{0,3}^{3,0}\left(\frac{3R_{Ons}^2}{8l_{eh}^3(\hbar\omega)}\middle| -\frac{3}{2}, -10\right),$$

where $G_{pq}^{mn}\left(z|_{b_1,\cdots,b_q}^{a_1,\cdots,a_p}\right)$ is the Meijer G function, $R_{Ons} = \frac{e^2}{4\pi\varepsilon_0\varepsilon_{st}k_BT}$ is the Onsager radius, $l_{eh}(\hbar\omega) = \sqrt{l_e^2(E_e) + l_h^2(E_h)}$ is the mean distance between the electron and the hole after thermalization, and $f(r, l_{eh}(\hbar\omega)) = \frac{3\sqrt{6}r^2}{\sqrt{\pi}l_{eh}^3(\hbar\omega)} \exp\left(-\frac{3r^2}{2l_{eh}^2(\hbar\omega)}\right)$ is the Gaussian distribution of distances $r$ after thermalization. Thermalization length for electron $l_e(E_e)$ (and hole $l_h(E_h)$) can be estimated for parabolic electron energy dispersion law and single LO phonon mode as:

$$l_e^2(E_e) \approx \frac{8}{9}a_B^2\left(\frac{\tilde{\varepsilon}}{m_e^*/m_0}\right)^2 \tanh\left(\frac{\hbar\Omega_{LO}}{2k_BT}\right)\left(\frac{E_e}{\hbar\Omega_{LO}}\right)^3 / \ln\left(\frac{4E_e}{\hbar\Omega_{LO}}\right),$$

where $a_B$ is the Bohr radius, $m_0$ is the free electron mass, $m_e^*$ is the electron effective mass, $\tilde{\varepsilon} = (n^{-2} - \varepsilon_{st}^{-1})$ is the lattice part of effective dielectric permittivity ($\varepsilon_{st}$ is the static dielectric permittivity, $n$ – refraction index), $\hbar\Omega_{LO}$ is the optical phonon energy. The functions $p(\hbar\omega)$ for $ZnWO_4$ and $MgWO_4$ were calculated using all required parameters, which are presented in Table 2. The distribution of excess photon energy ($\hbar\omega - E_g$) between electron and hole kinetic energies was taken in inverse proportion to their effective masses. The results of the calculation are presented in Fig. 2a. $MgWO_4$ is characterized by higher probability of geminate e–h recombination in comparison to $ZnWO_4$. The difference is connected with the reduced thermalization length in $MgWO_4$, which is due to higher effective masses of electrons and holes.

**Table 2**
Properties of $ZnWO_4$ and $MgWO_4$, which were used for the numerical simulation.

| | $ZnWO_4$ | $MgWO_4$ |
|---|---|---|
| $m_e^*/m_0$ [25] | 1.59 | 2.84 |
| $m_h^*/m_0$ [25] | 2.54 | 6.25 |
| $\varepsilon_{st}$ [26] | 16.1 | 18.0 |
| $n$ [22,27] | 2.1 | 2.03 |
| $\hbar\Omega_{LO}$ (eV) [28] | 0.1 | 0.1 |

As it was shown for the case of $ZnWO_4$ the excitation spectra of STE emission provides with information on the probability of exciton creation from geminate e–h pairs and can be compared to the calculated $p(\hbar\omega)$ [20]. The stochastic recombination of e–h pairs has low probability because the e–h pairs, which escape the Onsager sphere, can be captured by the impurities presented in each of the studied samples (Table 1). These impurities act as a radiative (e.g., impurity of Mo) or non-radiative relaxation channels, which are competitive to the STE. Therefore we expect that in the studied samples the excitation spectra of STE emission are mainly defined by the recombination of geminate e–h pairs and can be simulated in the energy region from the bandgap energy $E_g$ and up to the threshold of multiplication of electronic excitations (11–12 eV). The excitation spectra of STE emission are presented in Fig. 3 for $ZnWO_4$, $MgWO_4$ and for solid solution $Zn_{0.8}Mg_{0.2}WO_4$. The spectra are normalized to the intensity of the first excitation peak, which is connected with the direct creation of STE. The intensity of excitation spectrum is higher for $MgWO_4$ in comparison to $ZnWO_4$ in the region 4–11 eV (see Fig. 3, inset). This result is in compliance with the simulation of $p(\hbar\omega)$ (Fig. 2a) for these crystals, demonstrating the applicability of the simulation for the analysis of excitation spectra. The efficiency of the energy transfer to the emission centers in this case is mainly determined by the probability of exciton creation by geminate e–h pairs.

Higher light output of $ZnWO_4$ in comparison to $MgWO_4$ for X-ray excitation requires additional explanation. Nevertheless, experimental data (Fig. 3) and numerical simulation (Fig. 2a) demonstrate the higher probability of recombination of geminate e–h pairs for $MgWO_4$. Therefore the higher light output can be expected for $MgWO_4$ also under high-energy excitation. One of the possible explanations of this contradiction can be due to the differences in energy band structure between $ZnWO_4$ and $MgWO_4$. The bandgap energy $E_g$ for $MgWO_4$ is higher than that of $ZnWO_4$ by 0.4 eV [29]. The bandgap difference is manifested in the excitation

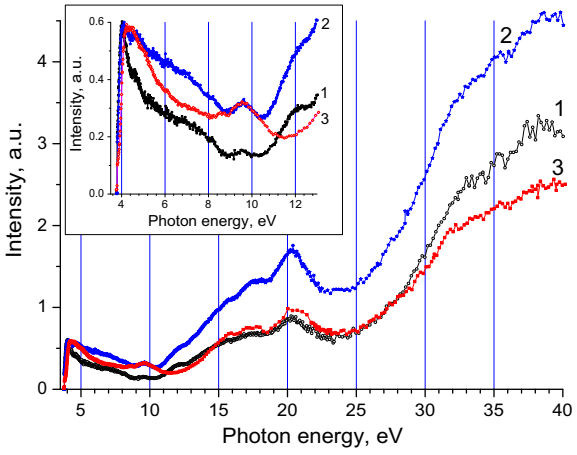


**Fig. 3.** Luminescence excitation spectra of $Zn_xMg_{1-x}WO_4$ for $x = 1$ (curve 1), 0.8 (2) and 0 (3) measured with synchrotron radiation, $\lambda_{em} = 500$ nm. In the inset – enlarged energy region from the fundamental absorption edge up to the photon multiplication region of $Zn_xMg_{1-x}WO_4$.

spectra as the shift of the low-energy threshold at ~4 eV and of the threshold of multiplication of electronic excitations at 11–12 eV to higher energies with the substitution of Zn with Mg cation (Fig. 3). This means that the mean energy for creation of one electron–hole pair is higher for $MgWO_4$ in comparison with $ZnWO_4$. Another feature of the energy bands structure is the presence of 3d states of Zn at the bottom of the valence band of $ZnWO_4$ [12,13], resulting in the increase of the density of states at the bottom of the valence band. On the contrary, Mg cation states do not participate in the formation of the valence band of $MgWO_4$. The presence of Zn 3d states at the bottom of valence band will change the energy distribution of secondary electrons and holes within the energy bands after the inelastic scattering of high energy electrons. It will redistribute the kinetic energy of secondary electrons and holes, with production of electrons with lower kinetic energy and holes with higher kinetic energy in $ZnWO_4$ in comparison with $MgWO_4$. Taking into account the higher mobility of electrons in comparison with holes, we expect the lower mean distance between thermalized electrons and holes in $ZnWO_4$ for the high-energy excitation. Experimental data for the high VUV excitation energies ($E_{ex}$ > 27 eV) also manifest this supposition. The excitation spectrum of $MgWO_4$ has lower intensity in comparison with $ZnWO_4$ (Fig. 3) at this energy region. This supposition can explain the lower light output for $MgWO_4$ for X-ray excitation (Fig. 1, inset).

Fig. 3 shows that the intensity of $Zn_{0.8}Mg_{0.2}WO_4$ excitation spectrum is even higher than of $ZnWO_4$ and $MgWO_4$. This result implies the higher efficiency of exciton creation from geminate e–h pairs in solid solution in comparison with pure compounds. According to the presented model such behavior can be caused by the decrease of the thermalization length in solid solutions. We have simulated the modification of $p(\hbar\omega)$for the case of reduction of the thermalization length. The curves of $p(\hbar\omega)$ calculated for the case of thermalization length $l_{eh}$ for $ZnWO_4$ and also for $l_{eh}/2$ and $l_{eh}/10$ are presented in Fig. 2b. This simulation demonstrates that the decrease of thermalization length leads to the increase of recombination probability. We observe this behavior for the solution with $x = 0.8$. It indicates that for solutions with $0 < x < 1$ the thermalization length is shorter than that for both $ZnWO_4$ and $MgWO_4$. In the region above the threshold of multiplication of electronic excitations the inelastic scattering of hot electrons and holes leads to creation of additional low-energy e–h pairs the thermalization length of which would be also smaller in the solid solution. This decrease of thermalization length in $Zn_{0.8}Mg_{0.2}WO_4$ results in the enhanced intensity of its excitation spectrum in comparison with pure materials in the high-energy VUV region and finally results in the enhanced light output for X-rays.

The excitation spectra have been measured in the UV-region for the complete set of the studied samples (Fig. 4). Gradual increase of the exciton recombination probability is manifested in the excitation spectra with the decrease of $x$ from 1 to 0.5 (Fig. 4a). Inverse trend is observed when $x$ decreases from 0.5 to 0 (Fig. 4b). Presented data also show the thermalization length modification in $Zn_xMg_{1-x}WO_4$ with the lowest value for $x = 0.5$. This result correlates with the highest value of X-ray light output, which is observed for the sample with $x = 0.5$.

The reasons for the decrease of thermalization length in solid solutions require additional study. The precise calculation of $p(\hbar\omega)$ for solid solutions is not possible since not all parameters are known. We may suppose that this effect is due to higher effective masses of electrons and holes in solid solutions in comparison with $ZnWO_4$ and $MgWO_4$. Unfortunately the band structure calculations for these solid solutions are not available at the present time. Also another reason for the decrease of mean distance between thermalized electrons and holes can be proposed. The non-uniform distribution of the components of solid solution result in the spatial fluctuation of the bottom of the conduction band and the top of the valence band (please note that the difference of the bandgaps of $ZnWO_4$ and $MgWO_4$ is about 0.4 eV). The local dips will appear on the bottom of conduction band and on the top of valence band. These spatial fluctuations of the bands are not significant for kinetic energies of carriers higher than 0.4 eV, but for lower energies the fluctuations would restrict the possible diffusion of thermalized electrons and holes. The amplitude of such fluctuations should be the highest for the equal concentration of Zn and Mg in the solid solution ($x = 0.5$). It will result in the decrease of the distance between the geminate electrons and holes and thus the probability of exciton formation would increase. These preliminary considerations should be confirmed by the further development of the model of recombination of geminate pairs with account for spatial fluctuations of component's distribution.

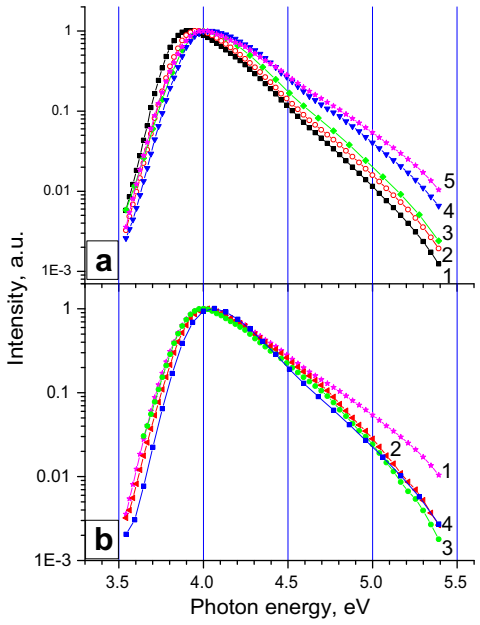


**Fig. 4.** (a) Luminescence excitation spectra of $Zn_xMg_{1-x}WO_4$ for $x = 1$ (curve 1), 0.8 (2), 0.7 (3), 0.6 (4), 0.5 (5), $\lambda_{em} = 500$ nm. (b) Luminescence excitation spectra of $Zn_xMg_{1-x}WO_4$ for $x = 0.5$ (curve 1), 0.4 (2), 0.3 (3), 0 (4) and 0 (6) measured in UV region, $\lambda_{em} = 500$ nm. Spectra were not corrected with the instrument function.

## 4. Conclusions

The light output of $Zn_xMg_{1-x}WO_4$ solid solutions as a function of composition is shown to have a maximum at $x = 0.5$. It is also demonstrated that at the same time the distance between thermalized electrons and holes has a minimum for the same value of $x$. It enhances the probability of geminate e–h pairs recombination and results in the observed increase of the light output. Presented results allow to consider $Zn_xMg_{1-x}WO_4$ as a new and promising scintillating material.

## Acknowledgements

We acknowledge the financial support from Mobilitas ESF program (Grants MTT83 and MJD219), Estonian Research Council – Institutional Research Funding IUT02-26, RFBR 11-02-01506-a grant and the support from the Baltic Science Link project coordinated by the Swedish Research Council, VR. We are grateful to Dr. A. Kotlov for his assistance during experiments at the SUPERLUMI

station. We are grateful to Dr. V. Nagirnyi for providing opportunity to perform the measurements of decay curves.

## References

[1] A.N. Belsky, E. Auffray, P. Lecoq, C. Dujardin, N. Garnier, H. Canibano, C. Pedrini, A.G. Petrosyan, IEEE Tran. Nucl. Sci. 48 (2001) 1095–1100.
[2] O. Sidletskiy, V. Kononets, K. Lebbou, S. Neicheva, O. Voloshina, V. Bondar, V. Baumer, K. Belikov, A. Gektin, B. Grinyov, M.-F. Joubert, Mater. Res. Bul. 47 (2012) 3249–3252.
[3] O. Sidletskiy, A. Belsky, A. Gektin, S. Neicheva, D. Kurtsev, V. Kononets, C. Dujardin, K. Lebbou, O. Zelenskaya, V. Tarasov, K. Belikov, B. Grinyov, Cryst. Growth Des. 12 (2012) 4411–4416.
[4] Y. Wu, D. Ding, S. Pan, F. Yang, G. Ren, J. Alloys Compd. 509 (2011) 366–371.
[5] K. Kamada, T. Endo, K. Tsutumi, T. Yanagida, Y. Fujimoto, A. Fukabori, A. Yoshikava, J. Pejchal, M. Nikl, Cryst. Growth Des. 11 (2011) 4484–4490.
[6] G. Gundiah, G. Bizarri, S. Hanrahan, M. Weber, E. Bourret-Courchesne, S. Derenzo, Nucl. Instrum. Methods Phys. Res., Sect. A 652 (2011) 234–237.
[7] V.S. Levushkina, D.A. Spassky, M.S. Tret'yakova, in: Book of Abstracts of 3rd International Conference Engineering of Scintillation Materials and Radiation Technologies (ISMART 2012), Dubna, Russia, 19–23 November, 2012, pp. 34–35.
[8] A. Gektin, N. Shiran, V. Shlyahturov, A. Belsky, in: Proceedings of the International Conference on Inorganic Scintillators and their Applications (SCINT95), Delft, The Netherlands, 28 August – 1 September, 1995, pp. 415–418.
[9] N.N. Ryskin, P. Dorenbos, C.W.E. van Eijk, S.Kh. Batygov, J. Phys.: Condens. Matter 6 (1994) 10423–10434.
[10] P. Dorenbos, J. Lumin. 134 (2013) 310–318.
[11] J.M. Ogieglo, A. Katelnikovas, A. Zych, T. Justel, A. Meijerink, C.R. Ronda, J. Phys. Chem. A 117 (2013) 2479–2484.
[12] O.Y. Khyzhun, V.L. Bekenev, V.V. Atuchin, E.N. Galashov, V.N. Shlegel, Mater. Chem. Phys. 140 (2013) 588–595.
[13] A. Kalinko, A. Kuzmin, R.A. Evarestov, Solid State Commun. 149 (2009) 425–428.
[14] S.G. Nedilko, Yu.A. Hizhnyi, T.N. Nikolaenko, Phys. Status Solidi (a) 2 (2005) 481–484.
[15] J. Ruiz-Fuertes, S. Lopez-Moreno, J. Lopez-Solano, D. Errandonea, A. Segura, R. Lacomba-Perales, A. Munoz, S. Radescu, P. Rodriguez-Hernandez, M. Gospodinov, L.L. Nagornaya, C.Y. Tu, Phys. Rev. B 86 (2012) 125202.
[16] P. Belli, R. Bernabei, F. Cappella, R. Cerulli, F.A. Danevich, S. d'Angelo, A. Incicchitti, V.V. Kobychev, D.V. Poda, V.I. Tretyak, J. Phys. G: Nucl. Part. Phys. 38 (2011) 115107.
[17] F.A. Danevich, D.M. Chernyak, A.M. Dubovik, B.V. Grinyov, S. Henry, H. Kraus, V.M. Kudovbenko, V.B. Mikhailik, L.L. Nagornaya, R.B. Podviyanuk, O.G. Polischuk, I.A. Tupitsyna, Yu. Ya, Vostretsov, Nucl. Instrum. Methods Phys. Res., Sect. A 608 (2009) 107–115.
[18] G. Zimmerer, Rad. Meas. 42 (2007) 859–864.
[19] T. Balasubramanian, B.N. Jensen, S. Urpelainen, B. Sommarin, U. Johansson, M. Huttula, R. Sankari, E. Nõmmiste, S. Aksela, H. Aksela, R. Nyholm, AIP Conf. Proc. 1234 (2010) 661–664.
[20] N.R. Krutyak, V.V. Mikhailin, A.N. Vasil'ev, D.A. Spassky, I.A. Tupitsyna, A.M. Dubovik, E.N. Galashov, V.N. Shlegel, A.N. Belsky, J. Lumin. 144 (2013) 105–111.
[21] V.B. Mikhailik, H. Kraus, Phys. Status Solidi B 247 (2010) 1583–1599.
[22] I. Bavykina, G. Angloher, D. Hauff, M. Kiefer, F. Petricca, F. Probst, Opt. Mater. 31 (2009) 1382–1387.
[23] R. Kirkin, V.V. Mikhailin, A.N. Vasil'ev, IEEE Trans. Nucl. Sci. 59 (2012) 2057–2064.
[24] A.N. Vasil'ev, V.V. Mikhailin, I.V. Ovchinnikova, Izvestiya Akademii nauk SSSR, sserya fizicheskaya 49 (1985) 2044–2048 (in Russian); Translated. in: Bulletin of the Academy of Sciences of the USSR. Physical Series 49 (1986) 164–168.
[25] S. Curtarolo, W. Setyawan, S. Wang, J. Xue, K. Yang, R.H. Taylor, L.J. Nelson, G.L.W. Hart, S. Sanvito, M. Buongiorno-Nardelli, N. Mingo, O. Levy, Comput. Mater. Sci. 58 (2012) 227–235.
[26] F.P. Emmenegger, H. Roetschi, J. Phys. Chem. Solids 32 (1971) 787–790.
[27] P.S. Mamykin, N.A. Batrakov, Trudy Uralskogo Politehnicheskogo Instituta Iss. 150 (1966) 101–111.
[28] G.M. Clark, W.P. Doyle, Spectrochim. Acta 22 (1966) 1441–1447.
[29] V.N. Kolobanov, I.A. Kamenskikh, V.V. Mikhailin, I.N. Shpinkov, D.A. Spassky, B.I. Zadneprovsky, L.I. Potkin, G. Zimmerer, Nucl. Instrum. Methods Phys. Res. 486/1–2 (2002) 496–503.